Eur. Phys. J. Plus (2019) **134**: 284
DOI 10.1140/epjp/i2019-12708-9

THE EUROPEAN PHYSICAL JOURNAL PLUS

Regular Article

Quantum thermometry by single-qubit dephasing

Sholeh Razavian[1], Claudia Benedetti[2], Matteo Bina[2,a], Yahya Akbari-Kourbolagh[1], and Matteo G.A. Paris[2]

[1] Faculty of Physics, Azarbaijan Shahid Madani University, Tabriz, Iran
[2] Quantum Technology Lab, Dipartimento di Fisica "Aldo Pontremoli", Università degli Studi di Milano, I-20133 Milano, Italy

Received: 16 January 2019 / Revised: 13 March 2019
Published online: 25 June 2019

Abstract. We address the dephasing dynamics of a qubit as an effective process to estimate the temperature of its environment. Our scheme is inherently quantum, since it exploits the sensitivity of the qubit to decoherence, and does not require thermalization with the system under investigation. We optimize the quantum Fisher information with respect to the interaction time and the temperature in the case of Ohmic-like environments. We also find explicitly the qubit measurement achieving the quantum Cramér-Rao bound to precision. Our results show that the conditions for optimal estimation originate from a non-trivial interplay between the dephasing dynamics and the Ohmic structure of the environment. In general, optimal estimation is achieved neither when the qubit approaches the stationary state, nor for full dephasing.

1 Introduction

Thermometry is the art of inferring the temperature of a (large) sample by reading its value on a (smaller) probe. Standard thermometry is based on the zeroth law of thermodynamics: the sample is assumed to have a large heat capacity whereas the probe (*i.e.* the thermometer) has a much smaller one. They are put in contact, and after a while they achieve thermalization by exchanging energy. The sample has not changed its temperature, owing to its large heat capacity, whereas the thermometer is now at the same temperature of the sample, which may be measured by the experimenter. In practice, since the heat capacity of the sample is always finite, a temperature measurement always implies a disturbance of the temperature itself. Besides, for any quantum system with a non-vanishing gap, precise thermometry cannot be achieved below a certain threshold temperature [1, 2].

Quantum probes, exploited as quantum thermometers, may offer a different and more effective avenue to thermometry. In turn, the use of quantum probes and quantum measurements for thermometry has attracted much attention [3, 4], with coherence and interference effects playing a relevant role [5–12]. Quantum probes offer the possibility of sensing temperature with small disturbance [13, 14], *i.e.* leaving the thermal system mostly unperturbed. In this framework, single-qubit probes are perhaps the best choice, being the simplest and smallest system suitable to extract information from the sample [15, 16]. Besides, it is of interest to exploit estimation scheme not based on the zeroth law of thermodynamics, *i.e.* on the exchange of energy between the sample and the thermometer [17, 18]. In this paper, we address in details the dephasing dynamics of a qubit as an effective process to estimate the temperature of its environment. This kind of scheme is inherently quantum, since it exploits the fragility and the sensitivity of quantum systems to decoherence, and does not require thermalization between the qubit probe and the system under investigation.

Indeed, the temperature of a quantum system is not a quantum observable. In other words, in a quantum setting temperature maintains its thermodynamical meaning, but it loses its operational definition. Therefore, any strategy aimed to determine temperature ultimately reduces to a parameter estimation problem, more precisely to a *quantum parameter estimation* problem [19]. The scope of quantum estimation is to provide an estimate of the unknown parameter from repeated measurements on the probe. The experimenter chooses a quantum measurement on the probe and then process the data. The choice of an estimator corresponds to a classical post processing of the outcomes after the measurement, whereas the choice of the measurement is the central problem of quantum metrology, since different measurements lead to different precisions. Indeed, quantum parameter estimation has been successfully applied to a variety of topics, ranging from phase estimation [20–23] and open system dynamics [24, 25], to quantum measurements in qubit chains [26, 27] and quantum phase transitions [28–30].

[a] e-mail: matteo.bina@gmail.com

In order to achieve optimal quantum thermometry, *i.e.* an estimator with minimum fluctuations, we will use notions and tools from quantum estimation theory. Notice, however, that we are not discussing here fluctuations of temperature in the thermodynamical sense. As a matter of fact, the temperature of the sample itself may not fluctuate [15]. On the other hand, the inferred value of temperature, *i.e.* the temperature estimate extracted from measurements performed on the qubit, does indeed fluctuate [31,32].

Concerning the interaction model, we assume that the interaction of the qubit with the sample is described by a dephasing Hamiltonian. The model is exactly solvable [33,34] when the environment (*i.e.* the sample under investigation) is excited in a thermal state. We let the qubit interact with its environment, and then we perform a measurement in order to extract information about the temperature. Our scheme is valid for a generic sample without any restriction on its energy spectrum. However, for the sake of providing some quantitative results, we assume an Ohmic spectral density with a generic Ohmicity parameter [35–42]. The interaction time is a free parameter, which we employ to maximize the qubit quantum Fisher information, *i.e.* the information about the temperature encoded in the state of the qubit as a result of the interaction with the sample. As we will see, the optimal interaction time is finite, *i.e.* the qubit is not required to approach its stationary state, nor it corresponds to a full dephasing. Rather, it is determined by a non-trivial interplay between the dephasing dynamics and the Ohmic structure of the environment [43–46], especially at low temperature.

The paper is structured as follows. In sect. 2, we briefly review the tools of local quantum estimation theory (QET), whereas in sect. 3 we describe in some details our physical model, and how we exploit QET techniques in our system. In sect. 4 we illustrate our results and show how to achieve optimal estimation with feasible measurements. Section 5 closes the paper with some concluding remarks.

2 Local quantum estimation theory

A parameter estimation scheme is a procedure in which a quantity of interest, say the parameter T, is not measured directly, but rather inferred by processing the data from the measurement of a different observable, say X, which may directly be measured on the system under investigation. We denote by $p(x|T)$ the conditional distribution of the outcomes of X, when the true value of the parameter is T, and by $\hat{T}(\mathbf{x})$, $\mathbf{x} = \{x_1, x_2, \ldots, x_M\}$ any *estimator*, *i.e.* a function mapping the M observed outcomes to a value of the parameter. The estimated value of the parameter is the average value of the estimator

$$\bar{T} = \int \mathrm{d}\mathbf{x}\, p(\mathbf{x}|T)\, \hat{T}(\mathbf{x}), \tag{1}$$

whereas the overall precision of the estimation procedure is quantified by its variance

$$\mathrm{Var}\, \hat{T} = \int \mathrm{d}\mathbf{x}\, p(\mathbf{x}|T)\, [\hat{T}(\mathbf{x}) - \bar{T}]^2. \tag{2}$$

In both equations $p(\mathbf{x}|T) = \Pi_{k=1}^{M}\, p(x_k|T)$, since measurements are performed on repeated preparations of the system and thus are independent. As a matter of fact, the variance of any unbiased estimator (*i.e.* an estimator for which $\bar{T} \to T$ in the asymptotic limit $M \gg 1$) for the parameter T is bounded by the Cramér-Rao inequality, stating that

$$\mathrm{Var}\, \hat{T} \geq \frac{1}{MF(T)}\,, \tag{3}$$

where $F(T)$ is the so-called Fisher information of the measurement of X, which is given by

$$F(T) = \int \mathrm{d}\mathbf{x}\, p(\mathbf{x}|T)\, [\partial_T \log p(\mathbf{x}|T)]^2\,, \tag{4}$$

where ∂_T denotes the derivative with respect to the parameter T. The optimal measurement for the parameter T is the measurement with the largest Fisher information, whereas an *efficient* estimator is an estimator saturating the Cramér-Rao inequality. The combination of the optimal measurement with an efficient estimator provides an optimal estimation scheme for the parameter T.

The maximization over all the possible quantum measurements may be indeed performed. The corresponding Fisher information is usually referred to as the *Quantum Fisher Information* (QFI) $H(T)$ [47–49]. The ultimate precision allowed by quantum mechanics is thus achieved by an estimator that saturates the quantum Cramér-Rao bound

$$\mathrm{Var}\, \hat{T} \geq \frac{1}{MH(T)}\,. \tag{5}$$

The expression of the QFI can be obtained from the quantum state of the system, and in particular from its eigenstates and eigenvectors, which contain the dependence on the parameter. Starting from the diagonal form of the density matrix describing the state of the system

$$\varrho_T = \sum_n \rho_n |\phi_n\rangle\langle\phi_n|, \tag{6}$$

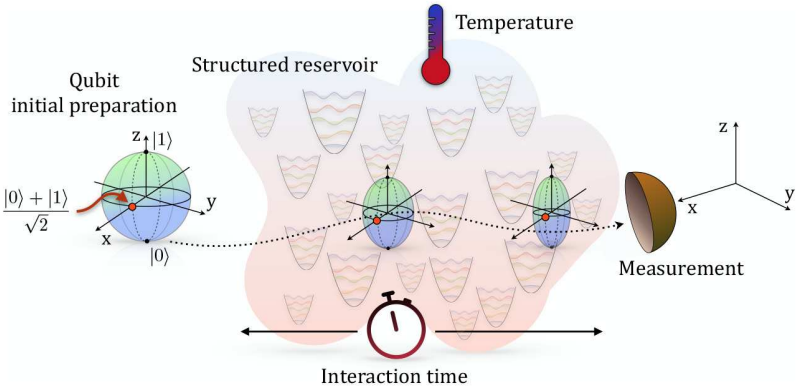

Fig. 1. Quantum thermometric scheme based on a single two-level system undergoing dephasing due to the interaction with a structured reservoir at thermal equilibrium. The dephasing mechanism is represented as a shrinking of the Bloch sphere (in interaction picture). After interaction a measurement of the optimal spin direction is performed.

the QFI is given by

$$H(T) = \sum_p \frac{(\partial_T \rho_p)^2}{\rho_p} + 2 \sum_{n \neq m} \frac{(\rho_n - \rho_m)^2}{\rho_n + \rho_m} |\langle \phi_n | \partial_T \phi_m \rangle|^2. \tag{7}$$

The first term in eq. (7) depends on how the eigenvalues of state depends on the parameter and it is referred to as the *classical* part of QFI, whereas the second term is referred to as the *quantum* part, and takes into account the dependence of eigenvectors on the parameter of interest. We point out that the local QET presented so far, dependent on the specific value of the parameter T, implicitly assumes a prior rough knowledge of the parameter of interest [19].

In order to quantify estimability of a parameter independently of its value, one may introduce the signal-to-noise ratio (SNR) $R_T = T^2/\operatorname{Var}\hat{T}$, which is larger for better estimators. Upon using the quantum Cramér-Rao inequality we have the bound

$$R_T \leq Q_T \equiv T^2 H(T), \tag{8}$$

where Q_T is usually referred to as the quantum signal-to-noise ratio (QSNR). The larger is QSNR the more effectively estimable is the parameter T.

In the following, we will exploit the framework described above in order to estimate the temperature T of a structured sample with Ohmic spectral density. The estimation strategy involves a qubit interacting with the sample for a certain interaction time that is then measured in order to infer the temperature. In particular, we investigate whether an effective quantum thermometric scheme may be achieved by considering a (exactly solvable) dephasing interaction model for the qubit. To this aim, we evaluate the optimal interaction time to achieve the maximum QFI and compute the corresponding QSNR. As we will see, we have encouraging numerical results in all the considered cases, and also few analytic results in the super-Ohmic regime, for low temperature in Ohmic environment, and in the high temperature regime for all the spectral densities.

3 Quantum thermometry by dephasing

Any interaction between a quantum system and its environment modifies the phases between the different components of its wave function. This usually produces dephasing [50,51] and, in turn, decoherence, due to the interaction among the system and the different modes of the thermal bath. This mechanism may be exploited to make the quantum system an effective probe to estimate parameters of the environment, without undermining the energy of the involved systems. In particular, in fig. 1, we illustrate a schematic diagram of our probing strategy for quantum thermometry by qubit dephasing. The dephasing mechanism is represented as a shrinking of the Bloch sphere, where the spin state (red dot) is in the interaction picture. After interacting with the sample (see discussion in sect. 4) the probe is measured in the optimal spin direction.

The qubit interacts with a structured reservoir at thermal equilibrium, characterized by a spectral density of Ohmic type. The total Hamiltonian can be written as (we set $\hbar = 1$ and the Boltzmann constant $k_B = 1$)

$$\mathcal{H} = \frac{1}{2}\omega_0 \sigma_z + \sum_k \omega_k b_k^\dagger b_k + \sigma_z \sum_k (g_k b_k^\dagger + g_k^* b_k), \tag{9}$$

where ω_0 is the probe transition frequency between the ground state $|0\rangle$ and the excited state $|1\rangle$, ω_k are the frequencies of the reservoir modes, $b_k(b_k^\dagger)$ is the bosonic annihilation (creation) operator for mode k and g_k are the coupling constants of each mode with the qubit, which can be distributed according to different spectral densities.

The qubit probe is initially prepared in a pure state $|\psi\rangle = \cos\frac{\theta}{2}|0\rangle + \sin\frac{\theta}{2}|1\rangle$ and the environment is supposed to be in an equilibrium thermal state at temperature T, namely $\varrho_B = \exp\{-\mathcal{H}_B/T\}/\mathcal{Z}$, with $\mathcal{Z} = \mathrm{Tr}[\exp\{-\mathcal{H}_B/T\}]$ the partition function and $\mathcal{H}_B$ the Hamiltonian of the bath. Going to the interaction picture, the reduced open system dynamics of the probe is governed by the map

$$\varrho_S(t) = \mathrm{Tr}_B\left[U_I(t)\,\varrho_{SB}(0)\,U_I^\dagger(t)\right], \tag{10}$$

where $U_I(t)$ is the interaction-picture evolution operator and $\rho_{SB}(0) = |\psi\rangle\langle\psi| \otimes \varrho_B$ is the initial state of the whole system.

Upon explicitly performing the trace over the degrees of freedom of the environment in eq. (10) the evolved density matrix of the probe at time t may be written as

$$\varrho_S(t) = \begin{pmatrix} \cos^2\frac{\theta}{2} & \frac{1}{2}e^{-\Gamma(T,t)}\sin\theta \\ \frac{1}{2}e^{-\Gamma(T,t)}\sin\theta & \sin^2\frac{\theta}{2} \end{pmatrix}, \tag{11}$$

where the time-dependent behavior of the off-diagonal terms depends on the decoherence factor

$$e^{-\Gamma(T,t)} = \sum_k \langle \exp(g_k b_k^\dagger - g_k^* b_k)\rangle, \tag{12}$$

where $\langle\,\bullet\,\rangle = \mathrm{Tr}[\bullet\,\varrho_B]$ is the average over the thermal state of the bath ϱ_B. The decoherence factor $\Gamma(T,t)$ depends on the temperature and on the spectral distribution of the coupling frequencies of the bath, which is quantified by the spectral density $J(\omega)$. The spectral density, in the continuous limit of the bath modes and for Ohmic-like distributions, is given by

$$J(\omega) \equiv J_s(\omega,\omega_c) = \frac{\omega^s}{\omega_c^{s-1}}\,e^{-\omega/\omega_c}, \tag{13}$$

where ω_c is the cutoff frequency and s is the Ohmicity parameter, which allows to classify the structured environment into three main classes, *i.e.* sub-Ohmic ($s < 1$), Ohmic ($s = 1$) and super-Ohmic ($s > 1$). The corresponding decoherence factors are, thus, given by

$$\Gamma(T,t) = \int \mathrm{d}\omega\, J(\omega)\,\frac{1-\cos\omega t}{\omega^2}\coth\left(\frac{\omega}{2T}\right), \tag{14}$$

where all the physical quantities in this equation should be considered dimensionless and rescaled with the cutoff frequency ω_c. Upon expanding the hyperbolic cotangent as $\coth(x) = 1 + 2\sum_{n=1}^{\infty}\mathrm{e}^{-2nx}$ we may write

$$\Gamma(T,t) = \Gamma(0,t) + 2\sum_{n=1}^{\infty} a_n^{1-s}\,\Gamma\left(0,\frac{t}{a_n}\right), \quad a_n \equiv a_n(T) = 1 + \frac{n}{T}, \tag{15}$$

where

$$\Gamma(0,t) = \int_0^\infty \mathrm{d}\omega \frac{1-\cos(\omega t)}{\omega^2}\,J(\omega) = \left(1 - \frac{\cos[(s-1)\arctan t]}{(1+t^2)^{\frac{s-1}{2}}}\right)\Gamma[s-1], \tag{16}$$

$\Gamma[z]$ being the Euler Gamma function. Notice that for $s \to 1$ we have $\Gamma(0,t) \xrightarrow{s\to 1} \frac{1}{2}\log(1+t^2)$. Upon substituting this expression in eq. (15), one realises that the series may be analytically evaluated, leading to

$$\Gamma(T,t) = \Gamma(0,t) + s(s-1)T^{s-1}\frac{\Gamma[s-1]^2}{\Gamma[s+1]}\left[2\zeta(s-1,1+t) - \zeta(s-1,1+t-iT) - \zeta(1+T+iT)\right], \tag{17}$$

where $\zeta(p,z) = \sum_{n=0}^{\infty}(z+n)^{-p}$ is the generalised (Hurwitz) Zeta function. Using this expression, one can see that the decoherence factor is a monotonically increasing function of time t for $s \leq 1$ whereas it saturates to a constant value for $s > 1$.

Given the decoherence factor, one may evaluate the QFI for the family of qubit states in eq. (11) [42], showing the optimal initial preparation corresponds to $\theta = \frac{\pi}{2}$. The explicit expression of the QFI, in this case, is given by

$$H(T,t) = \frac{[\partial_T\Gamma(T,t)]^2}{e^{2\Gamma(T,t)} - 1}\,. \tag{18}$$

Thanks to the scaling properties of $\Gamma(T,t)$, the QFI, and in particular its optimized value at the optimal interaction time t_{opt}, depends only on the Ohmicity parameter s of the sample under investigation and on its temperature T. Notice that using eq. (17) an analytic expression may be derived for the QFI, which is however rather cumbersome and it will not be reported here.

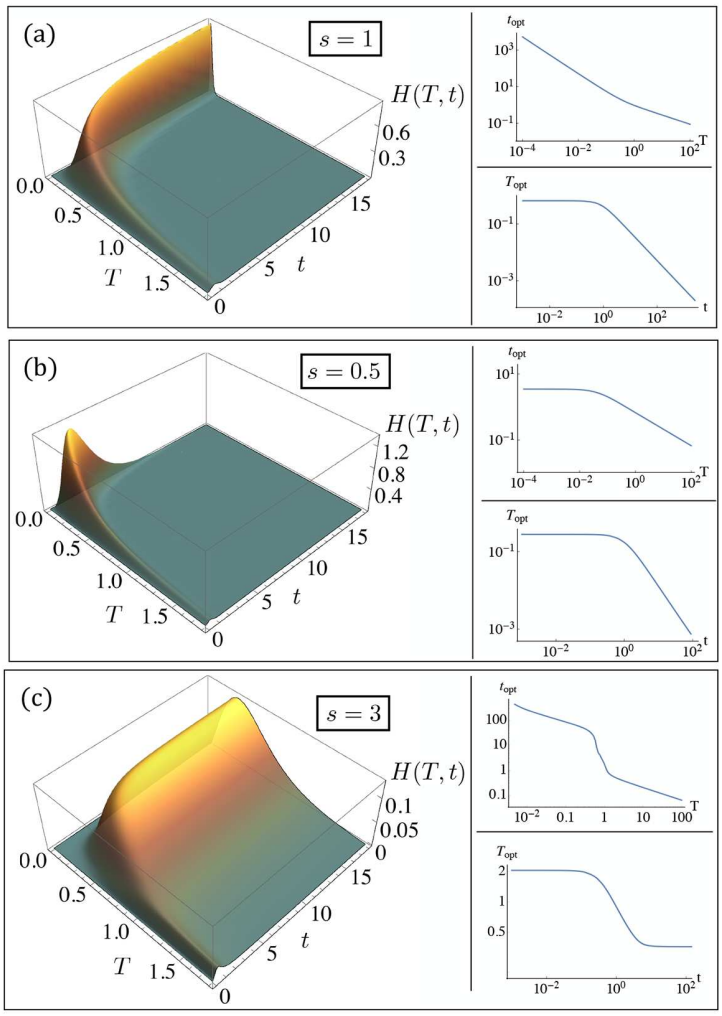

Fig. 2. The left boxes in each panel show plots of the QFI $H(T,t)$ as a function of temperature and time for three illustrative cases of (a) Ohmic ($s = 1$), (b) sub-Ohmic ($s = 0.5$) and (c) super-Ohmic ($s = 3$) environments. In the upper-right boxes we plot the optimal interaction times $t_{\rm opt}$ as a function of reservoir temperature T. In the lower-right boxes, we plot the temperature $T_{\rm opt}$ at which the QFI is maximized, as a function of the interaction time t.

4 Quantum thermometry of Ohmic-like samples

In the following, we consider quantum thermometry of different samples having spectral density belonging to the Ohmic family. In particular, we consider three specific values of the Ohmicity parameter, corresponding to paradigmatic examples of sub-Ohmic ($s = 0.5$), Ohmic ($s = 1$) and super-Ohmic ($s = 3$) environments. The behaviour of the QFI and the results of its maximization are shown in fig. 2. In the left boxes of each panel, we show a three-dimensional plot of $H(T,t)$, the QFI as a function of temperature T and time t. As it is apparent from the plots, at fixed temperature for $s = 1$ and $s = 0.5$, there is a maximum for the QFI as a function of time, whereas in the super-Ohmic case $s = 3$ we see maxima for high temperature, whereas in the low temperature regime we see saturation of the QFI, without a single local maximum value at a specific time. When a maximum for the QFI exists, it means that optimal estimation of temperature may be achieved at a finite interaction time $t_{\rm opt}$, *i.e.* before the qubit has reached its stationary state.

The right boxes of each panel in fig. 2 show two plots for each value of the Ohmicity parameter. In the upper ones we show the optimal interaction time $t_{\rm opt}$, *i.e.* the time at which the QFI reaches its maximum value, for a fixed value of the reservoir temperature. The different slopes in the plots identify different thermal regimes, say of *low* and *high* temperatures. At low temperature the optimal time is larger, while for increasing temperature it progressively decreases. This behaviour may have been intuitively expected given the nature of the probing technique. Indeed, the ability of the probe to extract information about the temperature of the environment comes from its fragility against decoherence. At low temperature, decoherence is weaker and it takes time to imprint information on the probe, while

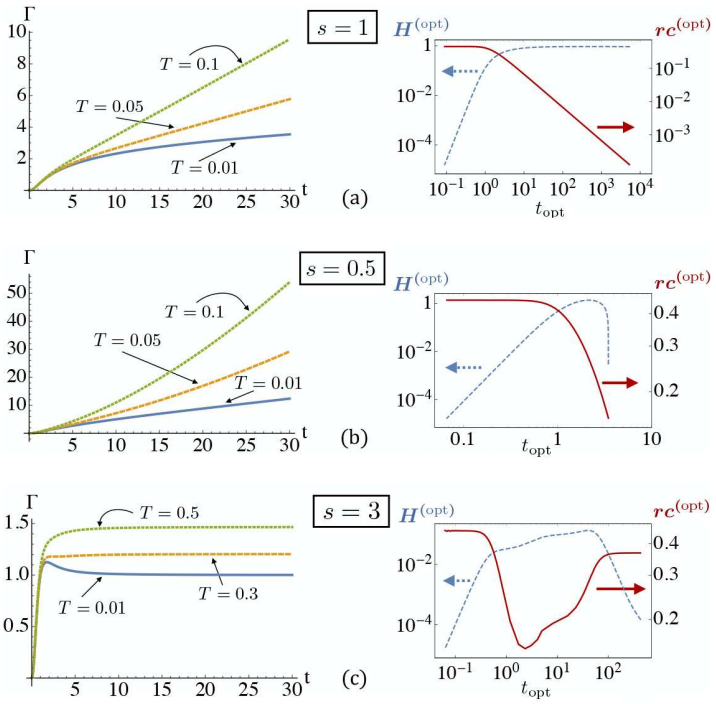

Fig. 3. On the left: plots of the decoherence factor $\Gamma(T,t)$ as a function of the interaction time t for three values of the reservoir temperature (see solid, dashed and dotted curves). On the right: plots of the QFI $H^{(\mathrm{opt})}$ (dashed curve) and the residual coherence $rc^{(\mathrm{opt})}$ (solid curve), both evaluated at the optimal time t_{opt}. We notice that in order to reach high values of the QFI the probe must interact enough time with the reservoir, which, inevitably, brings the qubit to lose coherence (right plots). The reason for this is the monotonic increase of the decoherence factor with time (left plots). Three characteristic types of structured environment have been analyzed, namely, (a) Ohmic ($s = 1$), (b) sub-Ohmic ($s = 0.5$) and (c) super-Ohmic ($s = 3$) reservoir.

at high temperature decoherence is faster. Notice also that at high temperature decoherence is mostly due to thermal fluctuations and the structure of the environment is no longer relevant. This is reflected in the behaviour of the QFI at high temperature, which is similar for the three values of s. On the contrary, the structure of the environment is crucial to determine the decoherence mechanism at low temperature, and this corresponds to a strongly s-dependent behaviour of the QFI (see also the discussion below on the quantum signal-to-noise ratio and fig. 4). The lower plots show the values T_{opt}, *i.e.* the temperature maximizing the QFI at a given interaction time t. This is a relevant quantity to consider in the case of *small samples*, where the interaction time may be indeed limited, especially when a traveling qubit is employed as a quantum probe.

The behavior of the decoherence factor $\Gamma(T,t)$ is illustrated in the left panels of fig. 3 for the three Ohmic regimes as a function of the interaction time t and for three different values of the reservoir temperature. In the large interaction time limit, *i.e.* when the qubit reaches its stationary state, the decoherence factor for both sub-Ohmic and Ohmic environments increases with time for all temperatures. This means that full decoherence is expected in these cases. On the other hand, for the super-Ohmic environment, the decoherence factor approaches a constant value, and a residual coherence in the qubit state is thus expected.

Motivated by this different behaviour, let us now compare the values of the maximum QFI to those of the residual coherence [52], as quantified by the sum of the absolute values of the off-diagonal elements of the density matrix of the probe after the interaction with the reservoir, *i.e.*

$$rc = \sum_{j \neq k} \left| \varrho_{S,jk}(t) \right|. \tag{19}$$

In the right panels of fig. 3, we show the value $H^{(\mathrm{opt})}$ of the QFI at the optimal interaction time, together with the residual coherence $rc^{(\mathrm{opt})}$ at the same time. We notice that in order to achieve higher values of the QFI, the probe should interact for enough time with the reservoir and, in turn, lose coherence. On the other hand, optimal estimation does not necessarily correspond to the strong decoherence regime, since in that case no information may be left encoded in the qubit state. The optimal conditions for estimation are thus determined by an interplay between the features of the dephasing dynamics and the specific Ohmic structure of the environment, rather than from the sole structure of the interaction.

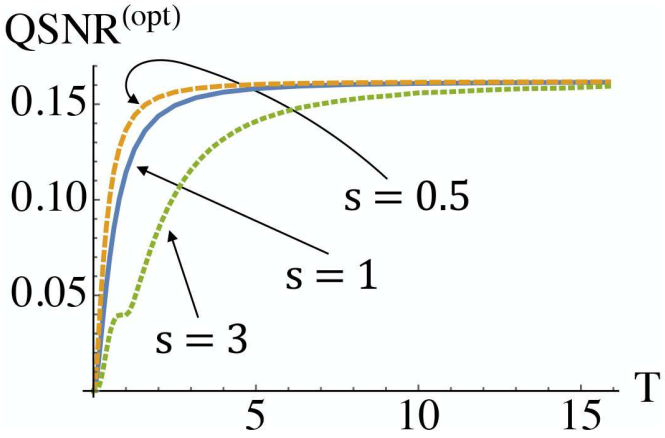

Fig. 4. Plot of the QSNR evaluated at the optimal interaction time $t_{\rm opt}$, as a function of the reservoir temperature T. We considered three classes of structured environments, Ohmic ($s = 1$), sub-Ohmic ($s = 0.5$) and super-Ohmic ($s = 3$).

Since this dephasing model is completely solvable at any time, it is reasonable to ask wether quantum non-Markovianity can be considered a resource for the estimation of the temperature. Non-Markovianity of the dephasing map has already been addressed, *e.g.* in refs. [51,53], where the authors demonstrate the existence of a critical value of the Ohmicity parameter above which memory effects occur, *i.e.* the dynamics is non-Markovian. This value is temperature-dependent and it is found to vary between $s = 2$ and $s = 3$ moving from zero to high temperature. The presence of non-Markovianity is witnessed by a decrease in time of the decoherence factor $\Gamma(T, t)$ of eq. (14). For example, referring to fig. 3, for $s = 3$ and $T = 0.01$ there exists a time interval where Γ decreases, a signature of non-Markovian dynamics. Only in the super-Ohmic regime at low temperatures memory effects arise. It follows that non-Markovianity cannot be linked to larger values of the QFI, so it cannot be considered a resource for temperature estimation.

The global estimability of temperature is addressed in fig. 4, where we show the QSNR evaluated at the optimal interaction time $t_{\rm opt}$, as obtained from eqs. (8) and (18). We show the QSNR for the three values of the Ohmicity parameter considered above. For low temperatures the QSNR is vanishing, meaning that in this regime the efficiency of any estimation procedure is very low. On the contrary, for higher temperatures it increases. The behavior is s-dependent in the intermediate temperature regime, whereas for high temperature, as already observed above, the structure of the environment becomes irrelevant, and the QSNR saturates to a universal value, independent of the nature of the spectral density of the environment.

We conclude this Section with few more analytic results, valid in some specific regimes. In the low temperature regime $T \ll 1$ and for Ohmic environment ($s = 1$) eq. (18) simplifies to

$$H(T,t) \overset{s=1}{=} \frac{\pi^2 t^2 [\pi t T \coth(\pi t T) - 1]^2}{(1+t^2)\sinh^2(\pi t T) - \pi^2 t^2 T^2}\,. \tag{20}$$

Upon comparing this expression with the numerical results we found that the above expression provides a good approximation for the temperature in the regime $T \lesssim 10^{-2}$. In the high temperature limit we obtain instead

$$H(T \gg 1, t) = \frac{4(K(t,s)-1)^2 \bar{\Gamma}[s-2]^2}{e^{-4T(1-K(t,s))\bar{\Gamma}[s-2]} - 1}\,, \quad s > 2, \tag{21}$$

where $K(t,s) = (1+t^2)^{1-\frac{s}{2}} \cos[(s-2)\arctan(t)]$.

5 Optimal measurement

Once the optimal estimation conditions have been determined, a question naturally arises on whether the corresponding bounds to precision may be achieved in practice, *i.e.* whether a feasible measurement exists whose Fisher information is equal to the quantum Fisher information [54,55].

In order to assess if this happens in our case, let us consider the most general projective measurement $\{M_\pm\}$, $M_+ + M_- = \mathbb{I}$ that can be performed on the qubit, and let us write the two projectors in the Bloch representation, *i.e.*

$$M_\pm = \frac{\mathbb{I} \pm \boldsymbol{a}\cdot\boldsymbol{\sigma}}{2}\,, \tag{22}$$

where $\boldsymbol{a} = [a_1, a_2, a_3]$, $\|\boldsymbol{a}\| = 1$ and $\boldsymbol{\sigma}$ consists of three 2×2 Pauli matrices, $\boldsymbol{\sigma} = [\sigma_x, \sigma_y, \sigma_z]$. Starting from the most general qubit state (11), the probability distribution of the two possibile outcomes is given by

$$p^{\pm}(t) = \mathrm{Tr}[\varrho_S(t)\, M_{\pm}] = \frac{1}{2}[1 \pm a_1 e^{-\Gamma} \sin\theta]\,, \tag{23}$$

corresponding to Fisher information

$$F(T) = \sum_{m=\pm} \frac{[\partial_T p^m(t)]^2}{p^m(t)}\,. \tag{24}$$

The above equation, with the prescription $\theta = \frac{\pi}{2}$ for the optimal state, makes it easy to see that for a measurement with $a_1 = 1$, *i.e.* the measurement of σ_x on the qubit, we have $F(T) = H(T)$ which corresponds to optimal estimation of temperature, provided that an efficient estimator is employed to process the data. Overall, we have that optimal temperature estimation at the quantum limit may be achieved by a feasible strategy, *i.e.* the preparation of the qubit in an eigenstate of σ_x and the measurement of the same observable after the interaction with the thermal sample.

6 Conclusions

In this paper we have addressed single-qubit quantum thermometry by dephasing and we have shown that it provides an effective process to estimate the temperature of Ohmic samples. Our scheme is inherently quantum, since it exploits the sensitivity of the qubit to decoherence, and does not require thermalization with the system under investigation.

We found that the QFI has a maximum as a function of time at any fixed temperature for Ohmic and sub-Ohmic samples, whereas in the super-Ohmic case this effect shows up only at high temperatures. In turn, this means that optimal estimation of temperature may be achieved at a finite interaction time, *i.e.* before the qubit has reached its stationary state. The only case in which the optimal estimation of the temperature coincides with stationarity and thermalization is for super-Ohmic environments in the low-temperature regime, where a saturation effect is observed. We also found that in order to achieve higher values of the QFI the probe should interact long enough with the sample and thus, roughly speaking, lose *enough coherence* in order to gain information about temperature. On the other hand, optimal estimation does not necessarily correspond to the strong decoherence regime, since in that case no information may be left encoded in the qubit state. Our results thus show that the optimal conditions for estimation are determined by a non-trivial interplay between the features of the dephasing dynamics and the specific Ohmic structure of the environment. Moreover, we pointed out that non-Markovianity does not play any role in the temperature estimation protocol, since it is only present in the dynamics of a probe interacting with a super-Ohmic environment at low temperature, with no enhancement of the estimation precision.

Finally, we have shown that optimal temperature estimation at the quantum limit may be achieved by a feasible strategy, involving preparation of the qubit in an eigenstate of σ_x, observable which is then measured after the interaction with the thermal sample. Our results also pave the way for future developments, including the use of entangled probes and, possibly, a suitable engineering of the interaction Hamiltonian. From the perspective of possible realizations of our probing scheme, there are several physical platforms implementing a dephasing dynamics of a two-level system in structured environments. We just mention atomic impurities embedded in Bose-Einstein condensates [56,57] and superconducting qubits [58,59].

This work has been supported by JSPS through FY2017 program (grant S17118) and by SERB through the VAJRA award (grant VJR/2017/000011). MGAP is member of GNFM-INdAM and thanks Francesca Gebbia for useful discussions.

References

1. M.G.A. Paris, J. Phys. A **49**, 03LT02 (2016).
2. P.P. Hofer, J.B. Brask, N. Brunner, *Fundamental limits on low-temperature quantum thermometry*, arXiv:1711.09827v3.
3. J. Goold, M. Huber, A. Riera, L. del Rio, P. Skrzypczyk, J. Phys. A **49**, 143001 (2016).
4. S. Vinjanampathy, J. Anders, Contemp. Phys. **57**, 545 (2016).
5. T.M. Stace, Phys. Rev. A **82**, 011611 (2010).
6. A. De Pasquale, T.M. Stace, *Quantum thermometry*, in *Thermodynamics in the Quantum Regime, Recent Progress and Outlook*, edited by F. Binder, L.A. Correa, C. Gogolin, J. Anders, G. Adesso (Springer, Berlin, 2018).

7. L.A. Correa, M. Mehboudi, G. Adesso, A. Sanpera, Phys. Rev. Lett. **114**, 220405 (2015).
8. S. Jevtic, D. Newman, T. Rudolph, T.M. Stace, Phys. Rev. A **91**, 012331 (2015).
9. T.H. Johnson, F. Cosco, M.T. Mitchison, D. Jaksch, S.R. Clark, Phys. Rev. A **93**, 053619 (2016).
10. S. Campbell, M.G. Genoni, S. Deffner, Quantum Sci. Technol. **3**, 025002 (2018).
11. W.K. Tham, H. Ferretti, A.V. Sadashivan, A.M. Steinberg, Sci. Rep. **6**, 38822 (2016).
12. L. Mancino, M. Sbroscia, I. Gianani, E. Roccia, M. Barbieri, Phys. Rev. Lett. **118**, 130502 (2017).
13. M. Brunelli, S. Olivares, M.G.A. Paris, Phys. Rev. A **84**, 032105 (2011).
14. M. Brunelli, S. Olivares, M. Paternostro, M.G.A. Paris, Phys. Rev. A **86**, 012125 (2012).
15. J. Gemmer, M. Michel, G. Mahler, *Quantum Thermodynamics*, in *Lecture Notes in Physics*, Vol. **784** (Springer-Verlag, Berlin, Heidelberg, 2004).
16. M. Horodecki, J. Oppenheim, Nat. Commun. **4**, 2059 (2013).
17. F. Seilmeier, M. Hauck, E. Schubert, G.J. Schinner, S.E. Beavan, A. Hogele, Phys. Rev. Appl. **2**, 024002 (2014).
18. F. Haupt, A. Imamoglu, M. Kroner, Phys. Rev. Appl. **2**, 024001 (2014).
19. M.G.A. Paris, Int. J. Quantum Inf. **7**, 125 (2009).
20. A.S. Holevo, Rep. Math. Phys. **16**, 385 (1979).
21. G.M. D'Ariano, C. Macchiavello, M.F. Sacchi, Phys. Lett. A **248**, 103 (1998).
22. M. Bina, A. Allevi, M. Bondani, S. Olivares, Sci. Rep. **6**, 26025 (2016).
23. A. Monras, Phys. Rev. A **73**, 033821 (2006).
24. M. Sarovar, G.J. Milburn, J. Phys. A **39**, 8487 (2006).
25. M.A.C. Rossi, M.G.A. Paris, Phys. Rev. A **92**, 010302(R) (2015).
26. D. Tamascelli, C. Benedetti, S. Olivares, M.G.A. Paris, Phys. Rev. A **94**, 042129 (2016).
27. J. Kiukas, K. Yuasa, D. Burgarth, Phys. Rev. A **95**, 052132 (2017).
28. P. Zanardi, M.G.A. Paris, L. Campos Venuti, Phys. Rev. A **78**, 042105 (2008).
29. M. Bina, I. Amelio, M.G.A. Paris, Phys. Rev. E **93**, 052118 (2016).
30. M.A.C. Rossi, M. Bina, M.G.A. Paris, M.G. Genoni, G. Adesso, T. Tufarelli, Quantum Sci. Technol. **2**, 01LT01 (2017).
31. C.H. Webster, *The Future of Quantum Roulette Noise Thermometry*, NPL Report DEM-TQD-007 (2006).
32. T. Jahnke, S. Lanery, G. Mahler, Phys. Rev. E **83**, 011109 (2011).
33. H.-P. Breuer, F. Petruccione, *The Theory of Open Quantum Systems* (Oxford University Press, New York, 2002).
34. M. Palma, K.-A. Suominen, A.K. Ekert, Proc. R. Soc. London Ser. A **452**, 567 (1996).
35. J. Paavola, J. Piilo, K.-A. Suominen, S. Maniscalco, Phys. Rev. A **79**, 052120 (2009).
36. R. Martinazzo, K.H. Hughes, F. Martelli, I. Burghardt, Chem. Phys. **377**, 21 (2010).
37. C.J. Myatt *et al.*, Nature (London) **403**, 269 (2000).
38. J. Piilo, S. Maniscalco, Phys. Rev. A **74**, 032303 (2006).
39. D. Tamascelli, A. Smirne, S.F. Huelga, M.B. Plenio, Phys. Rev. Lett. **120**, 030402 (2018).
40. A. Lemmer, C. Cormick, D. Tamascelli, T. Schaetz, S.F. Huelga, M.B. Plenio, New J. Phys. **20**, 073002 (2018).
41. M. Bina, F. Grasselli, M.G.A. Paris, Phys. Rev. A **97**, 012125 (2018).
42. C. Benedetti, F. Salary, M.H. Zandi, M.G.A. Paris, Phys. Rev. A **97**, 012126 (2018).
43. V. Cavina *et al.*, Phys. Rev. A **98**, 050101 (2018).
44. L.A. Correa *et al.*, Phys. Rev. A **96**, 062103 (2017).
45. H.J. Miller, J. Anders, Nat. Commun. **9**, 2203 (2018).
46. M. Mehboudi *et al.*, Quantum **2**, 66 (2018).
47. H. Cramer, *Mathematical Methods of Statistics* (Princeton University Press, Princeton, NJ, 1946).
48. C.W. Helstrom, *Quantum Detection and Estimation Theory* (Academic Press, NY, 1976).
49. S.L. Braunstein, C.M. Caves, Phys. Rev. Lett. **72**, 3439 (1994).
50. C. Benedetti, M.G.A. Paris, Int. J. Quant. Inf. **12**, 1461004 (2014).
51. C. Addis, G. Brebner, P. Haikka, S. Maniscalco, Phys. Rev. A **89**, 024101 (2014).
52. T. Baumgratz, M. Cramer, M.B. Plenio, Phys. Rev. Lett **113**, 140401 (2014).
53. P. Haikka, T.H. Johnson, S. Maniscalco, Phys. Rev. A **87**, 010103(R) (2013).
54. F. Chapeau-Blondeau, Phys. Rev. A **94**, 022334 (2016).
55. C. Benedetti, M.G.A. Paris, Phys. Lett. A **378**, 2495 (2014).
56. P. Haikka, S. McEndoo, G. De Chiara, G.M. Palma, S. Maniscalco, Phys. Rev. A **84**, 031602(R) (2011).
57. M.A. Cirone, G. De Chiara, G.M. Palma, A. Recati, New. J. Phys. **11**, 103055 (2009).
58. F. Yan *et al.*, Nat. Commun. **7**, 12964 (2016).
59. P.I. Villar, F.C. Lombardo, Phys. Lett. A **379**, 246 (2015).